Available online at www.sciencedirect.com
SCIENCE DIRECT
Journal of Power Sources 155 (2006) 239–245
JOURNAL OF POWER SOURCES
www.elsevier.com/locate/jpowsour

Thin inclusion approach for modelling of heterogeneous conducting materials

Nikolay Lavrov [a], Alevtina Smirnova [b,*], Haluk Gorgun [b], Nigel Sammes [b]

[a] *Davenport University, 4801 Oakman Boulevard, Dearborn, MI 48126, USA*
[b] *University of Connecticut, Department of Materials Science and Engineering, Connecticut Global Fuel Center, 44 Weaver Road, Unit 5233, Storrs, CT 06269, USA*

Received 31 March 2005; accepted 2 May 2005
Available online 26 July 2005

Abstract

Experimental data show that heterogeneous nanostructure of solid oxide and polymer electrolyte fuel cells could be approximated as an infinite set of fiber-like or penny-shaped inclusions in a continuous medium. Inclusions can be arranged in a cluster mode and regular or random order. In the newly proposed theoretical model of nanostructured material, the most attention is paid to the small aspect ratio of structural elements as well as to some model problems of electrostatics. The proposed integral equation for electric potential caused by the charge distributed over the single circular or elliptic cylindrical conductor of finite length, as a single unit of a nanostructured material, has been asymptotically simplified for the small aspect ratio and solved numerically. The result demonstrates that surface density changes slightly in the middle part of the thin domain and has boundary layers localized near the edges. It is anticipated, that contribution of boundary layer solution to the surface density is significant and cannot be governed by classic equation for smooth linear charge. The role of the cross-section shape is also investigated. Proposed approach is sufficiently simple, robust and allows extension to either regular or irregular system of various inclusions. This approach can be used for the development of the system of conducting inclusions, which are commonly present in nanostructured materials used for solid oxide and polymer electrolyte fuel cell (PEMFC) materials.

Keywords: Fuel cell; Gas diffusion medium; Thin conducting inclusion; Charge distribution; Heterogeneous structure

1. Introduction

The development of nanostructured and self-assembling materials attracted significant attention in various applications, such as energy storage and energy conversion devices. However, the main emphasis of nanoscale studies of nanomaterials has been made in the synthesis of these materials, rather than in the area of a rigorous theoretical approach. Thus, some of the existing experimental results, such as those related for example to exceptionally high ionic conductivity of yttria-stabilized zirconia ultrathin films [1] cannot be explained on the basis of existing mathematical models. Mathematical description in correlation with detailed structural characterization and information about transport properties of these materials could open new opportunities and significantly extend the area of their application.

A wide variety of nanostructured materials are commonly used for porous catalyst layers of solid oxide and polymer electrolyte fuel cells [2–6], self-assembling structures such as carbon aerogels [7], carbon nanotubes [8], gas diffusion layers [9,10], and gas separation membranes [11,12]. These materials can be assumed to be a combination of a series of conductive inclusions separated by a non-conductive gas medium.

Various mathematical approaches to heterogeneous structures have been suggested [13–15]. One of these applies a straightforward numerical solution of a 3D problem by means of finite element or boundary element (FE/BE) code. However, this approach is feasible only in the case of a single inclusion or a finite number of inclusions and is not robust when for a structural system of an unlimited number of inclu-

* Corresponding author. Tel.: +1 860 4868762; fax: +1 860 4868378.
E-mail address: alevtina@engr.uconn.edu (A. Smirnova).

0378-7753/$ – see front matter © 2005 Elsevier B.V. All rights reserved.
doi:10.1016/j.jpowsour.2005.05.058

sions. In the theory of elasticity it has been stated, that singular perturbation of a domain is one of the most critical issues for solving this problem numerically. Thus, a direct numerical technique is not robust when we consider a dynamic process in the medium with a singular perturbation.

Another widely used approach is based on the representative volume concept when "effective" homogeneous parameters of an heterogeneous material can be derived from "representative" volume, i.e. cubical domains containing a finite set of inclusions. This approach to a heterogeneous material allows one to derive constitutive equations of heterogeneous medium from obtained properties of the representative volumes.

The goal of this work was to develop a simple model of a thin conducting inclusion in a dielectric medium. In future, a complete theoretical model allowing rigorous predictions of the properties of nanostructured materials will be created on the basis of an asymptotic approach to a single conductive inclusion, proposed in our work. In addition, it should be emphasized, that the proposed asymptotic approach can be applied to a dielectric media containing systems of thin conducting inclusions with various positions, orientations, dimensions, configurations, curvilinear contours, and properties.

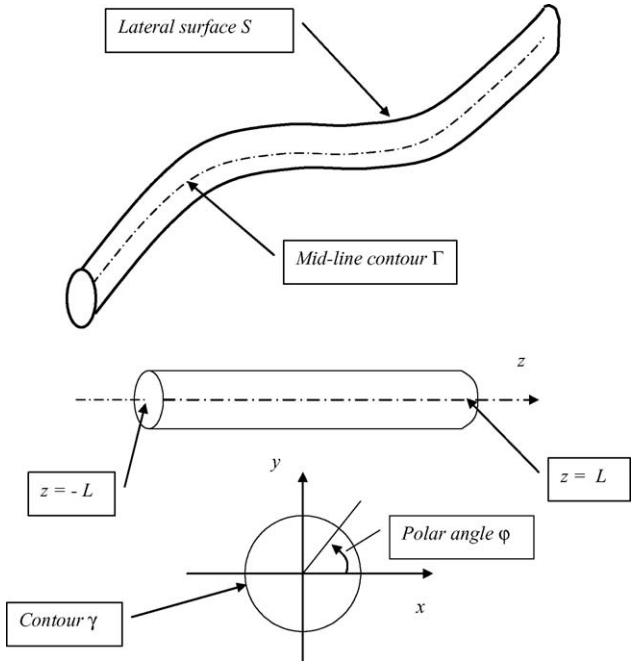

Fig. 1. Configuration of the conductor.

2. Model description

In order to solve the problem of a single cylindrical inclusion, an asymptotic simplification is used with the assumption that the aspect ratio (δ) of the inclusion is small, i.e. two transversal dimensions are much smaller than the length. The cross-section may differ from the circle; the electrostatic charge is distributed over the surface of the conductor. To derive an equation for the unknown density, the original integral equation for the potential is asymptotically simplified. The original 3D problem is decomposed into a combination of two problems of reduced dimension. The first one is governed by the integral equation for the unknown linear charge (net charge in the cross-section) over the axis of the conductor. The second one is a 2D electrostatic problem governed by the integral equation over the boundary contour of the cross-section. The derived asymptotic equations for the unknown density are valid at the points located far away from the edges.

In order to determine the charge density near the edge, the boundary layer equation is derived. Uniform circular and elliptic cylinders are used as examples. Results for a circular cylinder correlate well with classic results in the middle part of the domain; contribution of the boundary layer solution is significant near the ends; influence of cross-section shape is investigated.

2.1. Formulation of the electrostatic problem

The perfect conductor with a total electrostatic charge (Q) is placed into an infinite dielectric medium with dielectric constant ε. Charge is assumed to be distributed over the surface (S) of the conductor. Configuration of the conductor is shown in Fig. 1, where Γ is the mid-line contour (closed or unclosed), γ the boundary contour of the cross-section (contour γ can differ from the circle). The unknown surface density, ρ, of the charge is governed by the classic equation of electrostatics:

$$V = \frac{1}{4\pi\varepsilon} \iint_S \frac{\rho(x', y', z')\mathrm{d}S(x', y', z')}{\sqrt{(x-x')^2 + (y-y')^2 + (z-z')^2}}, \quad (2.1.1)$$

$$Q = \iint_S \rho(x', y', z')\,\mathrm{d}S(x', y', z'). \quad (2.1.2)$$

Here V stands for the electric potential of the conductor, x, y, z the Cartesian coordinates, and Q is the total charge.

Asymptotic analysis of the integral in the right-hand side of Eq. (2.2.1) has been conducted in potential theory (electrostatics/electrodynamics, acoustics, hydrodynamics, theory of thin aerofoil, and material science/composites) [3]. In this paper, we apply results obtained in asymptotic analysis of singular integrals to specific problem of electrostatics.

2.2. Axially symmetric problem

We consider first the electrostatic problem for a circular cylinder in the axially symmetrical electrostatic field. We use an integral equation (2.1.1) and assume that the edge area is negligible and the surface S means the *lateral* surface of the conductor. The density depends upon the axial coordinate z,

$\rho = \rho(z)$. Eq. (2.1.1) can be rewritten in the form:

$$V = \frac{a}{4\pi\varepsilon}\int_0^{2\pi}\int_{-L}^{L}\frac{\rho(z')\mathrm{d}z'\mathrm{d}\varphi}{\sqrt{(z-z')^2+4a^2\sin^2(\varphi/2)}}, \qquad (2.2.1)$$

φ stands for polar angle.

The unknown surface density is represented as a sum of the "smooth" part describing the density in the points far away from the ends, and two boundary layers localized near the ends $z = L$ and $z = -L$:

$$\rho(z) = q\left(\frac{z}{L}\right) + \Phi\left(\frac{L-z}{a}\right) + \Phi\left(\frac{L+z}{a}\right). \qquad (2.2.2)$$

$$\int_0^{\infty}\int_0^{2\kappa}\frac{\Phi(\tau')}{\sqrt{(\tau-\tau')^2+4\sin^2(\varphi/2)}}\mathrm{d}\tau'\,\mathrm{d}\varphi = -q(1)\int_0^{2\pi}\frac{\varphi\sin\varphi\,\mathrm{d}\varphi}{\sqrt{\tau^2+4\sin^2(\varphi/2)}\left[\tau+\sqrt{\tau^2+4\sin^2(\varphi/2)}\right]}. \qquad (2.2.5)$$

The smooth part is associated with the large scale L of a change in the variable z; the boundary layers correspond with the small scale a.

Equation for the smooth part $q(s)$ of the density is derived using the asymptotic integral equation assuming that $a \ll L - |z|$, $a \ll L$, $\delta = a/L \ll 1$:

$$\frac{2\varepsilon V}{a} = \int_{-1}^{1}\frac{q(s')-q(s)}{|s-s'|}\mathrm{d}s' + q(s)\left[\ln\frac{1-s^2}{\delta^2} - \frac{4}{\pi}\int_0^{\pi/2}\ln(\sin\varphi)\mathrm{d}\varphi\right], \qquad (2.2.3)$$

where $s = z/L$ a new dimensionlesss variable, small terms $O(\delta\ln\delta)$ are neglected. This equation is to be solved together with equality (2.1.2) at a given total charge Q. The derived asymptotic equation correlates very well with the classic equation of Pocklington [4] for a thin cylindrical conductor:

$$V = \frac{a}{2\varepsilon}\int_{-L}^{L}\frac{\rho(z')\mathrm{d}z'}{\sqrt{(z-z')^2+a^2}}. \qquad (2.2.4)$$

These equations are asymptotically equivalent, and differ in the negligible term $O(\delta\ln\delta)$. Eqs. (2.2.3) and (2.2.4) allow one to calculate "smooth" density at the points far-away from the ends. However, smooth density may contain some error near the ends of the conductor.

2.2.1. Equation of boundary layer near the edge

After solving Eq. (2.2.3) for the smooth part $q(s)$ of the density we can calculate density corrected for the boundary layer near the edge $z = L$. For the reason of symmetry, the boundary layer near the opposite edge $z = -L$ is assumed to be identical. We substitute the representation $\rho(z) = q(z/L) + \Phi((L-z)/a)$ into Eq. (2.2.1) under the assumption that a contribution of the boundary layer near the opposite end ($z = -L$) is negligible near the end $z = L$ under study. Thus, introducing a new "short" variable, $\tau = (L-z)/a$, we subtract Eq. (2.2.3) for a smooth part. After some asymptotic replacements and limit transition $\delta \to 0$, $1/\delta \to \infty$ we derive the boundary layer equation in the form:

2.3. Elliptic cylinder

Consider a cylindrical conductor with elliptic cross-section (ellipse γ). Let a and b ($b < a$) stand for semi-axes of the ellipse. Parameters a and b are of the same order (the aspect ratio $\kappa = b/a = O(1)$ and both are much smaller than the length $2L(a/L = o(1))$. Surface density ρ depends on the longitudinal coordinate z (associated with "long" scale L) and polar angle φ within the cross-section. Contour γ, polar angle φ and Cartesian coordinates x, y, and z are shown in Fig. 2.

Potential equation (2.1.1) can be written in the form:

$$V = \frac{1}{4\pi\varepsilon}\int_{\gamma}\mathrm{d}\gamma(\varphi')\int_{-L}^{L}\frac{\rho(\varphi',z')}{\sqrt{(z-z')^2+r^2(\varphi,\varphi')}}\mathrm{d}z';$$

$$r^2 = r^2(\varphi,\varphi') = a^2(\cos\varphi-\cos\varphi')^2 + b^2(\sin\varphi-\sin\varphi')^2 = 4\sin^2\left(\frac{\varphi-\varphi'}{2}\right)\left[a^2\sin^2\left(\frac{\varphi+\varphi'}{2}\right) + b^2\cos^2\left(\frac{\varphi+\varphi'}{2}\right)\right];$$

$$\mathrm{d}\gamma(\varphi') = \sqrt{a^2\sin^2\varphi' + b^2\cos^2\varphi'}\,\mathrm{d}\varphi'. \qquad (2.3.1)$$

First, we look for smooth surface density ρ and linear charge P (net charge in the cross-section) as functions of Cartesian

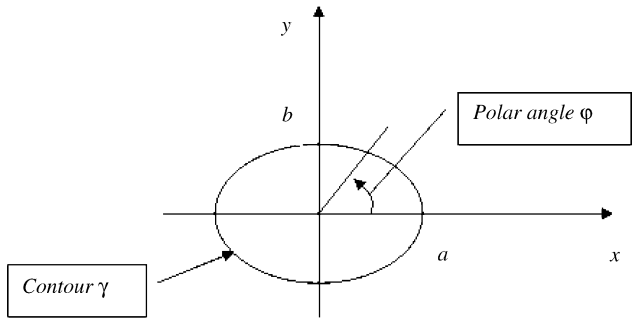

Fig. 2. Contour γ, polar angle φ, and Cartesian coordinates x, y, and z.

coordinates x, y, and z:

$$\rho = q\left(\frac{x}{a}, \frac{y}{a}, \frac{z}{L}\right);$$

$$P = P\left(\frac{z}{L}\right) = \int_\gamma \rho\left(\frac{x'}{a}, \frac{y'}{a}, \frac{z}{L}\right) \mathrm{d}y(x', y')$$

$$= \int_0^{2\pi} q\left(\cos\varphi', \frac{b}{a}\sin\varphi', \frac{z}{L}\right)\sqrt{a^2\sin\varphi' + b^2\cos\varphi'}\,\mathrm{d}\varphi'. \tag{2.3.2}$$

Further, we develop combined linear charge (T) including boundary layers localized near the ends in the form:

$$T(z) = P\left(\frac{z}{L}\right) + \Phi\left(\frac{L-z}{a}\right) + \Phi\left(\frac{L+z}{a}\right). \tag{2.3.3}$$

We are seeking the unknown linear charge $P(s)$ distributed along the z-axis ("smooth" part of solution), and charge distribution $q = q(x/a, y/a, s)$ over the contour γ (of the cross-section $z = \text{const}$). Then we analyze linear charge $T(z)$ as a function of "short scale" coordinate.

2.3.1. Asymptotic equation for the smooth density

First, we substitute this representation (2.3.2) for the density to Eq. (2.3.1) and derive the asymptotic of potential V:

$$4\pi\varepsilon V = \int_{-L}^{L} \frac{P(z'/L) - P(z/L)}{|z - z'|}\,\mathrm{d}z' + P\left(\frac{z}{L}\right)\ln\frac{4(L^2 - z^2)}{a^2}$$
$$- \int_\gamma q\left(\cos\varphi', \frac{b}{a}\sin\varphi', \frac{z}{L}\right)\ln[(\cos\varphi - \cos\varphi')^2$$
$$+ \kappa^2(\sin\varphi - \sin\varphi')^2]\mathrm{d}\gamma(\varphi'). \tag{2.3.4}$$

The structure of Eq. (2.3.4) gives an indication that we have to seek the density q in the degenerated form:

$$q\left(\cos\varphi, \frac{b}{a}\sin\varphi, \frac{z}{L}\right) = \Psi(\varphi)P\left(\frac{z}{L}\right);$$

$$\int_\gamma \Psi(\varphi')\mathrm{d}\gamma(\varphi') = 1. \tag{2.3.5}$$

Then we substitute (2.3.5) into (2.3.4) and achieve a system of four equations for four unknowns: $P(z/L)$, $\Psi(\varphi)$, V, and c.

$$4\pi\varepsilon V = \int_{-L}^{L} \frac{P(z'/L) - P(z/L)}{|z - z'|}\,\mathrm{d}z' + P\left(\frac{z}{L}\right)\ln\frac{4(L^2 - z^2)}{c^2};$$

$$2\ln a + \int_\gamma \Psi(\varphi')\ln[(\cos\varphi - \cos\varphi')^2$$
$$+ \kappa^2(\sin\varphi - \sin\varphi')^2]\mathrm{d}\gamma(\varphi') = 2\ln c;$$

$$\int_\gamma \Psi(\varphi')\mathrm{d}\gamma(\varphi') = 1; \qquad \int_{-L}^{L} P\left(\frac{z'}{L}\right)\mathrm{d}z' = Q. \tag{2.3.6}$$

Thus, separation of variables is completed. The first equation of the derived system contains information on 3D effects of the phenomenon under study. The second equation corresponds with the 2D electrostatic problem of charge distribution in a cylindrical conductor of infinite extent. It has a shortcoming of being a 2D formulation; 2D does not allow the evaluation of 3D effects, and of the determination of the net charge P in the cross-section. Unknown parameter c can be considered as some "effective" radius of circular cylinder with the same linear charge $P(z/L)$.

2.3.2. Boundary layer near the edge

After solving Eq. (2.3.6) for the linear charge $P(z/L)$ and angular distribution $\Psi(\varphi)$ we can calculate the correction to the linear charge P caused by the boundary layer near the edge $z = L$. This boundary layer is constructed under the assumption of validity of angular distribution of charge (within the cross-section) everywhere, including at the vicinity of this edge. We substitute representation $\rho(\varphi,z) = [P(z/L) + \Phi((L-z)/a)]\Psi(\varphi)$ into Eq. (2.3.1). (Contribution of the boundary layer localized near the opposite end $z = -L$ to the density near the end $z = L$ is negligible.) Then we incorporate the new "short" variable $\tau = (L - z)/a$ and subtract the first equation (2.3.7) for a smooth part $P(z/L)$ from Eq. (2.3.1). After some asymptotic replacements and limit transition $\delta \to 0$; $1/\delta \to \infty$ we obtain the boundary layer equation in the form:

$$\int_0^{2\pi} \Psi(\varphi')\mathrm{d}\gamma(\varphi') \int_0^\infty$$
$$\times \frac{\Phi(\tau')}{\sqrt{(\tau - \tau')^2 + (1 - \cos\varphi')^2 + \kappa^2(\sin\varphi)^2}}\mathrm{d}\tau' = P(1)\int_0^{2\pi}$$
$$\times \Psi(\varphi')\ln\frac{2\tau}{\tau + \sqrt{\tau^2 + (1 - \cos\varphi')^2 + \kappa^2(\sin\varphi')^2}}\mathrm{d}\gamma(\varphi'). \tag{2.3.7}$$

3. Results and discussion

High-resolution images of conductive heterogeneous structures are presented in Figs. 3 and 4. The micrographs indicate that cylindrical or almost cylindrical fibers are elements of the structure; the fibers within the structure can be assembled in three typical orders: tree-like order (cluster), chaotic order, and regular order. All these orders can be governed by asymptotic equations over the graph. The graph can be connected or contain fragments without connection with the main tree.

3.1. Circular cylinder

Equations for the smooth part and the boundary layer were solved numerically. Calculated dimensionless density and linear charge:

$$p(z) = \frac{2\pi aL\rho(z)}{Q} = \frac{2\pi aL\rho(z)}{\iint_S \rho(z')\mathrm{d}S(x', y', z')} \tag{3.1.1}$$

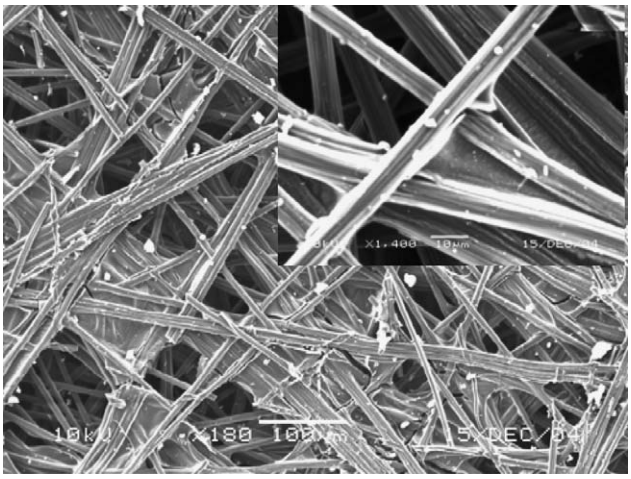

Fig. 3. Electrically conducting carbon paper used as a gas diffusion layer in PEMFCs; inset shows the same material at higher magnification.

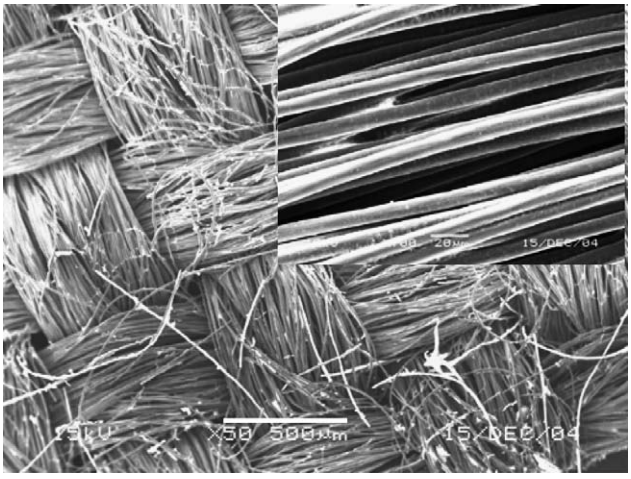

Fig. 4. Electrically conducting carbon cloth used as a gas diffusion layer in PEMFCs; inset shows the same material at higher magnification.

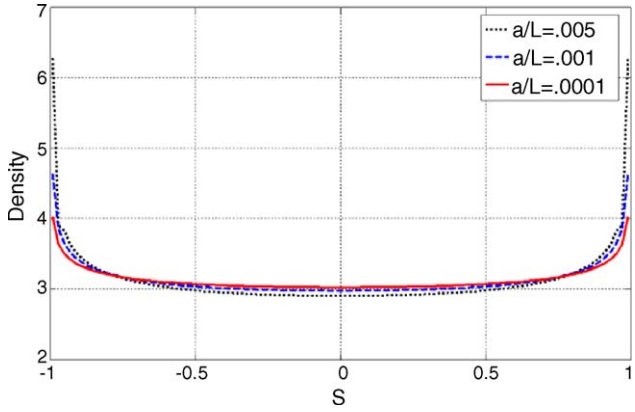

Fig. 5. Charge density calculated from equation of Pocklington at various aspect ratio ($a/L = 0.05$; 0.01; 0.001).

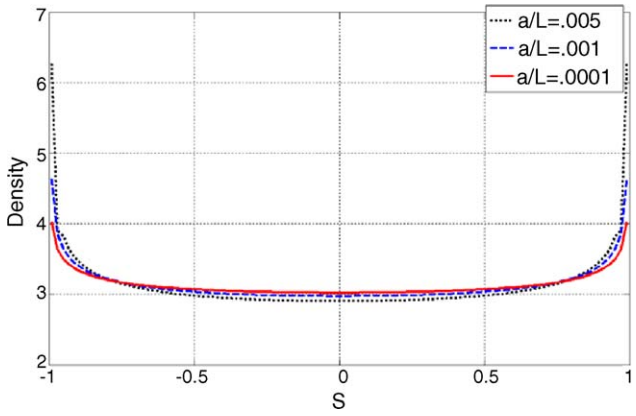

Fig. 6. Dimensionless density calculated from asymptotic equation at various aspect ratio ($a/L = 0.05$; 0.01; 0.001).

is presented in Figs. 5–7. Fig. 5 presents the density calculated from the equation of Pocklington at various aspect ratios ($a/L = 0.005$; 0.001; 0.0001). Fig. 6 presents the dimensionless density calculated from the asymptotic equation (2.2.3) (without boundary layer) at various aspect ratios ($a/L = 0.005$; 0.001; 0.0001). Comparison between the linear charge calculated from the equation of Pocklington (dotted line), Eq. (2.2.3) (solid line), and Eqs. (2.2.3) and (2.2.5) (dashed line) at $a/L = 0.05$ is presented in Fig. 7. Calculations indicate that linear charge in the middle part of the inclusion can be successfully calculated by means of asymptotic equation (2.2.3) for smooth density; these results correlate well with the classic integral equation (2.2.4). Calculations show that the boundary layer makes a significant contribution near the ends, and this fast change of density cannot be governed by the asymptotic equation for smooth density (2.2.3) or the equation of Pocklington. Results show that the boundary layer solution allows one to estimate high gradients of linear charge near the ends of the conductor. Effective zone of the boundary layer is about two diameters of the conductor.

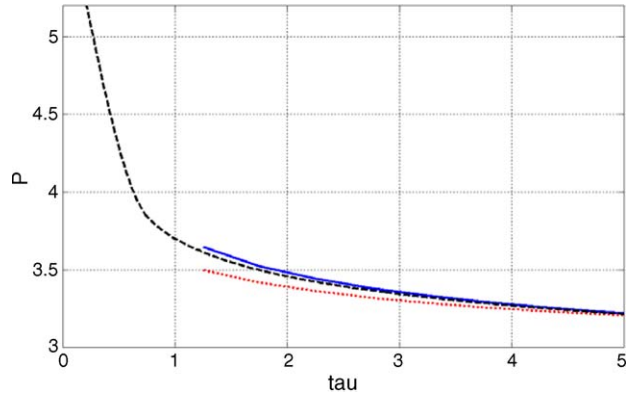

Fig. 7. Comparison between the linear charge calculated from equation of Pocklington (dotted line), Eq. (2.2.3) (solid line), and Eqs. (2.2.3) and (2.2.5) (dashed line) at $a/L = 0.05$.

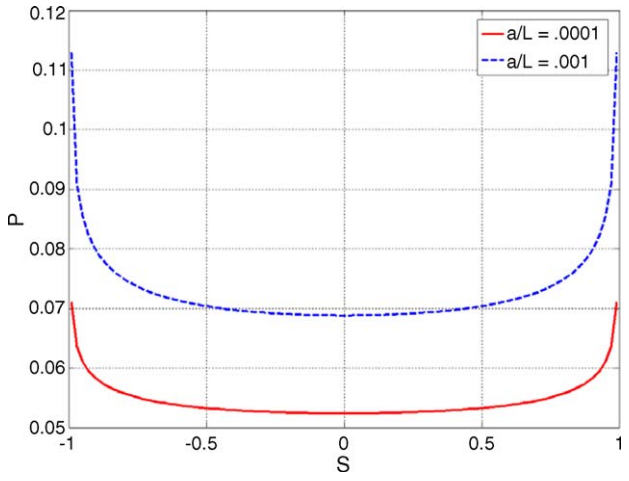

Fig. 8. The smooth linear charge at various aspect radii ($a/L = 0.001; 0.0001$) for elliptical cross-section $b/a = 2$.

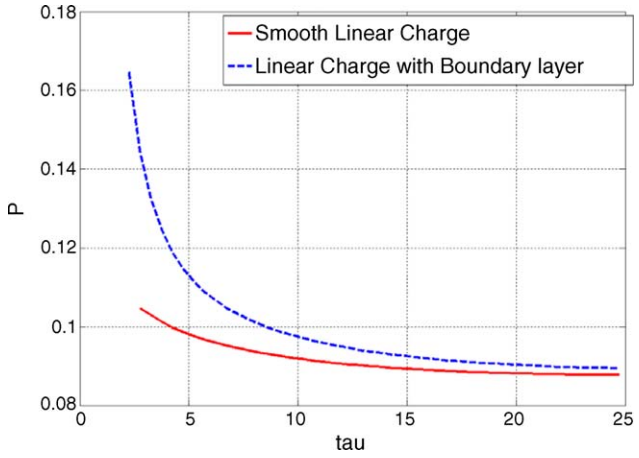

Fig. 10. Edge effect (solid line for smooth linear charge, dashed line for linear with boundary layer); calculations were conducted for $a/L = 0.05$ and $b/a = 2$.

3.2. Elliptic cylinder

Equations for the smooth part of the linear charge and boundary layer were solved numerically, and dimensionless linear charge $P(z/L)$ (containing smooth part and boundary layer):

$$\bar{P}(s) = \frac{L P(s)}{Q} \tag{3.2.1}$$

and angular distribution $\Psi(\varphi)$ of charge over the cross-section boundary contour were calculated. Fig. 8 presents the smooth linear charge at various aspect ratios ($a/L = 0.001;\ 0.0001$) for elliptical cross-section $b/a = 2$. Fig. 9 presents the angular distribution $\Psi(\varphi)$ for ellipses with ratio $b/a = 2$, 3, and 1 (circle). It should be noted that the classical approximation of Pocklington does not consider noncircular cross-sections. The edge effect is shown in Fig. 10 (solid line for smooth linear charge, dashed line for linear with boundary layer); calculations were conducted for $a/L = 0.05$ and $b/a = 2$. Results show that a high gradient of linear charge near the edge cannot be estimated without calculation of the boundary layer term. The effective zone of the boundary layer is about two to three diameters of the conductor.

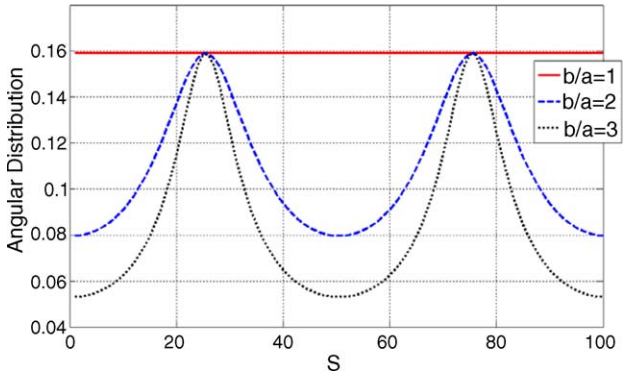

Fig. 9. The angular distribution $\Psi(\varphi)$ for ellipses with ratio $b/a = 2$, 3, and 1 (circle).

It should be noted that the 2D approach allows one to calculate the angular distribution of the electric charge over the cross-section boundary, but does not allow one to find the net charge in the cross-section $z = \text{const}$. Linear charge can be found from a 3D formulation, which can be asymptotically transformed to an integral equation over the axis of the conductor. A similar situation takes place in the analysis of thin films/thin-walled inclusions. In some specific cases a 1D approach to thin film/inclusion can meet principal trouble related to finiteness of inclusion in the plane or other reasons. This incorrectness of the boundary value problem of the reduced dimension sometimes appears to be an artifact. Correct formulation of the boundary value problem can be obtained on the basis of a 3D approach. 3D formulation can take into account the finite size of the inclusion in the plane, finite curvature of the median surface, non-uniform thickness effects, and the presence of additional scale parameter (with dimension of length) associated with the internal structure of the film. All the above-mentioned reasons make the 1D formulation insufficient, and requires a more detailed study. Reduction of dimension in the corresponding boundary value problem is still possible, but has to be implemented more thoroughly. Mathematical methods of this kind of reduction have already been developed in solid mechanics/acoustics. We assume that this advanced asymptotic technique can be successfully applied to the new thin film effects discovered in [5].

4. Conclusion

The electrostatic problem of a single cylindrical conducting inclusion for a SOFC catalyst layers has been solved using the asymptotic decomposition for a single rod-like conductor in a dielectric medium. It was shown that the surface distri-

bution of the charge can be described by the integral equation over the mid-line axis for an unknown linear charge and that this representation is valid at the points far from the ends of the conductor. In the case of straight or a curvilinear inclusion, the charge distribution near the ends is governed by a boundary layer equation. This effective technique is sufficient in describing a complex system of various inclusions, such as gas diffusion or electrode catalyst layers in PEMFCs, and a large number of non-identical conductors having different lengths, mid-line contours, and cross-section shapes, which is typical for ceramic electrically conductive porous materials.

As the next step, this approach will be incorporated in the complex model of heterogeneous nanostructured material containing a regular/irregular system of inclusions, which will allow the development of novel nanostructured materials. It has been shown, that derived asymptotic relations are simple enough and allow extension to heterogeneous medium associated with the system of inclusions, furthermore, the required level of accuracy is achieved. It should be emphasized, that the proposed novel approach results in prediction of the properties of heterogeneous material directly, without additional simplifying physical hypotheses.

References

[1] I. Kosacki, C. Rouleau, P. Becher, J. Bentley, D. Lowndes, Surface/interface-related conductivity in nanometer thick YSZ films, Electrochem. Solid-State Lett. 7 (12) (2004) 459–461.
[2] S. Litster, G. MLean, PEM fuel cell electrodes, J. Power Sources 130 (1–2) (2004) 61–76.
[3] S.M. Haile, Fuel cell materials and components, Acta Mater. 51 (19) (2003) 5981–6000.
[4] H. Yokokawa, T. Horita, N. Sakai, K. Yamaji, M.E. Brito, Y.-P. Xiong, H. Kishimoto, Protons in ceria and their roles in SOFC electrode reactions from thermodynamic and SIMS analyses, Solid State Ionics 174 (1–4) (2004) 205–221.
[5] V.V. Kharton, F.M.B. Marques, A. Atkinson, Transport properties of solid oxide electrolyte ceramics: a brief review, Solid State Ionics 174 (1–4) (2004) 135–149.
[6] W.Z. Zhu, S.C. Deevi, A review on the status of anode materials for solid oxide fuel cells, Mater. Sci. Eng. A 362 (1–2) (2003) 228–239.
[7] A. Smirnova, X. Dong, H. Hara, A. Vasiliev, N. Sammes, Novel carbon aerogel-supported catalysts for PEM fuel cell application, Int. J. Hydrogen Energy 30 (2) (2005) 149–158.
[8] N. Rajalakshmi, M.M. Hojin Ryu, S. Shaijumon, Ramaprabhu, Performance of polymer electrolyte membrane fuel cells with carbon nanotubes as oxygen reduction catalyst support material, J. Power Sources 140 (2) (2005) 250–257.
[9] Wei Sun, Brant A. Peppley, Kunal Karan. Modeling the Influence of GDL and flow-field plate parameters on the reaction distribution in the PEMFC cathode catalyst layer, J. Power Sources (2005) (available online).
[10] Th. Frey, M. Linardi, Effects of membrane electrode assembly preparation on the polymer electrolyte membrane fuel cell performance, Electrochim. Acta 50 (1) (2004) 99–105.
[11] Pratibha Pandey, R.S. Chauhan, Membranes for gas separation, Progr. Polym. Sci. 26 (6) (2001) 853–893.
[12] S.M. Saufi, A.F. Ismail, Fabrication of carbon membranes for gas separation—a review, Carbon 42 (2) (2004) 241–259.
[13] S. Torquato, Random Heterogeneous Materials: Microstructure and Macroscopic Properties, Series: Interdisciplinary Applied Mathematics, vol. 16, Springer-Verlag, New York, 2002.
[14] L.J. Gibson, M.F. Ashby, Cellular Solids: Structure and Properties, 2nd ed., Cambridge University Press, Cambridge, 2004.
[15] R. Bove, P. Lunghi, N. Sammes, SOFC mathematic model for systems simulations. Part 1. From a micro-detailed to macro-black-box model, Int. J. Hydrogen Energy 30 (2) (2005) 181–187.